Published in final edited form as:

Cancer Res. 2010 April 1; 70(7): 2819–2828. doi:10.1158/0008-5472.CAN-09-1915.

Tie2 signaling regulates osteoclastogenesis and osteolytic bone invasion of breast cancer

Yongfen Min[1], **Xiubao Ren**[1], **David B Vaught**[2], **Jin Chen**[2,3,4], **Edwin Donnelly**[5], **Conor C. Lynch**[2], and **P. Charles Lin**[1,2,3]

[1]Department of Radiation Oncology, Vanderbilt-Ingram Cancer Center, Vanderbilt University Medical Center, Nashville, TN 37232, USA.

[2]Department of Cancer Biology, Vanderbilt-Ingram Cancer Center, Vanderbilt University Medical Center, Nashville, TN 37232, USA.

[3]Department of Cell and Development Biology, Vanderbilt-Ingram Cancer Center, Vanderbilt University Medical Center, Nashville, TN 37232, USA.

[4]Department of Medicine, Vanderbilt-Ingram Cancer Center, Vanderbilt University Medical Center, Nashville, TN 37232, USA.

[5]Department of Radiology, Vanderbilt-Ingram Cancer Center, Vanderbilt University Medical Center, Nashville, TN 37232, USA.

Abstract

Breast to bone metastasis is a common occurrence in the majority of patients with advanced breast cancer. The metastases are often incurable, are associated with bone destruction and high rates of morbidity. Understanding the underlying mechanisms of how metastatic tumor cells induce bone destruction is critically important. We previously reported that Tie2, a receptor tyrosine kinase, is significantly increased in human breast cancer tissues compared to normal and benign breast tumors, and regulates tumor angiogenesis. In this study, we identify a new function of Tie2 in osteoclastogenesis and osteolytic bone invasion of breast cancer. Tie2 is present in hematopoietic stem/precursor cells. Genetic deletion of Tie2 or neutralization of Tie2 function using soluble Tie2 receptor impaired osteoclastogenesis in an embryonic stem (ES) cell differentiation assay. In contrast, deletion of Tie2 has no effect on osteoblastogenesis. As CD11b myeloid cells have the potential to become osteoclast and Tie2 is present in certain population of these cells, we isolated Tie2+ and Tie2 − myeloid cells. We observed a significant reduction of osteoclastogenesis in Tie2− compared to Tie2+ CD11b cells. Consistently, neutralization of Tie2 activity *in vivo* significantly inhibited osteolytic bone invasion and tumor growth in a mammary tumor model, which correlated with a significant reduction of osteoclast and tumor angiogenesis. Collectively, these data reveal a direct and novel role of Tie2 signaling in osteoclast differentiation. These findings identify Tie2 a therapeutic target for controlling not only tumor angiogenesis, but also osteolytic bone metastasis in breast cancer.

Keywords

Breast cancer; bone metastasis; Tie2; osteoclast; osteoclastogenesis

Address correspondence to: P. Charles Lin, Ph.D., Vanderbilt University Medical Center, 712 PRB, 2220 Pierce Ave, Nashville TN, 37232, Phone: 615-936-1749, Fax: 615-936-1872, Charles.lin@vanderbilt.edu.

Introduction

Bone metastasis is a serious medical problem, which is characterized as osteolytic or osteoblastic, and most patients with breast cancer have predominantly osteolytic lesions. In osteolytic metastasis, tumor cells produce factors that promote the differentiation and activation of the cells responsible for osteolysis, i.e. the osteoclast. In turn, bone resorption by osteoclasts releases growth factors from the bone matrix that enable tumor cells to grow and progress in the bone microenvironment. This reciprocal interaction between breast-cancer cells and the bone microenvironment forms a vicious cycle that increases both bone destruction and the tumor burden (1). In addition, osteoclast hyperactivation in metastatic sites results in destructive and painful lesions that are accompanied by pathological fracture, spinal compression, and hypercalcemia. Therefore targeting osteoclast differentiation and breaking the vicious cycle offers an effective means to combat bone metastasis.

Vascular endothelium plays important roles in metastasis, as tumor cells are transported through blood and lymphatic vascular systems, and direct interaction between tumor cells and the endothelium is essential for metastasis as tumor cells have to intravasate and extravasate during metastasis. Emerging evidence also indicates a connection between the endothelium and osteoclastogenesis. For example, angiogenesis is closely associated with increased osteoclast formation in multiple myeloma and other cancers, as well as inflammatory conditions, such as rheumatoid arthritis (2–4). Tie2 is a receptor tyrosine kinase expressed predominantly in vascular endothelium and regulates angiogenesis. We have reported a significant elevation of Tie2 in human breast cancer tissues compared to normal breast tissues (5). Neutralization of Tie2 function using a soluble Tie2 receptor significantly inhibited tumor angiogenesis and tumor growth in mammary tumors (6,7).

Osteoclasts are derived from hematopoietic stem cells (8,9). Since hematopoietic cells share a common progenitor with endothelial cells, it is no surprise that these two cell types often share common mediators. In addition to endothelium, Tie2 is also expressed in hematopoietic stem/progenitor cells and interaction of Tie2 in hematopoietic stem cells with angiopoietin-1, a ligand for Tie2, from osteoblasts control stem cell quiescence and survival in the bone marrow niche (10). Furthermore, over expression of angiopoietin-1 in transgenic mice results in an increase of bone volume and bone parameters compared with wild-type littermates (11). We have shown that blocking Tie2 activation prevented bone destruction in arthritis (12). These data support a role of Tie2 signaling in osteoclast differentiation and function.

In this study, we report a direct role of Tie2 signaling in osteoclastogenesis. Accordingly, neutralization of Tie2 function inhibited osteolytic bone invasion, tumor angiogenesis and tumor progression of breast cancer.

Material and Methods

Materials

Eight weeks old female Balb/c mice were purchased from Jackson Labs. The animals were housed in pathogen-free units at the Vanderbilt University Medical Center, in compliance with IACUC regulations. Adenoviral vectors directing the expression of GFP (AdGFP) and a soluble Tie2 inhibitor, ExTek, (AdExTek) (7) were used. The viral vectors were propagated in 293 cells and purified by CsCl gradients as described (7). The murine mammary tumor line, 4T1, was stably transfected with a luciferase construct (4T1/Luc) and used in the study.

In vitro osteoclastogenesis and osteoblastogenesis assays

Wild type mouse ES cells (TL1) and Tie2 knockout ES cells were kindly provided by the Vanderbilt Stem Cell Biology Core and Dr. Daniel Dumont at the Sunnybrook and Women's

Research Institute, respectively. The cells are maintained in the media in the presence of leukemia inhibitory factor (LIF, 1000 U/ml, Gibco) and passaged every other day as described (13). For induction of osteoclast differentiation, we used a published protocol (14). Recombinant ExTek protein (100ng/ml) was used to neutralize Tie2 activation in TL1 ES cell differentiation. Three weeks after induction of cell differentiation, TRAP staining was performed to detect activated osteoclasts according to manufacturer's instructions (Sigma) and multinucleated TRAP+ cells (2 or more nuclei per cell) were counted in randomly selected fields under microscopy. The experiment was done in triplicate, and repeated three times.

For induction of osteoblast differentiation, we followed a published protocol (15). Recombinant ExTek protein (100ng/ml) was used to neutralize Tie2 activation in TL1 ES cell differentiation. The complete program of differentiation usually takes place in 25–30 days. At the end of differentiation, mineralization is observed by Alizarin red (Sigma) staining (15). Positive stained cells were counted in randomly selected field under microscopy. All experiments were done in triplicate and repeated twice.

Osteoclastogenesis assays were also performed using myeloid cells from 8 weeks old Balb/c mice. CD11b+ cells were purified from mouse bone marrow using anti CD11b magnetic beads per manufacturer's instructions (Miltenyi Biotech). CD11b+ cells were subsequently stained with PE-labeled mouse anti-Tie2 antibody (eBioscience). Tie2+ and Tie2− myeloid cells were sorted with a FACStarPlus flow cytometer (Becton Dickinson, Franklin Lakes, NJ). $CD11b^{total}$, $CD11b^{Tie\text{-}2-ve}$ and $CD11b^{Tie\text{-}2+ve}$ were seeded (5×10^5) into 8-well chamber slides (Labtek) and exposed to RANKL (50ng/ml) and M-CSF (25ng/ml) in 10% serum containing α-MEM for 14 days with changes of media every 2–3 days. For Actin Ring Staining of osteoclasts, cells were fixed with 100% MeOH at −20°C for 10 minutes, and incubated with phalloidin (Invitrogen) for 1 hour at room temperature. Total multinucleated cells (with 3 or more nuclei per cell) were counted in each well and graphed. The experiment was performed as triplicate and repeated three times. Osteoclast differentiation ability was calculated as the fraction of plated cells that undergo osteoclast differentiation (output/input).

Cell proliferation assay

ES cells were incubated with recombinant ExTek protein or BSA control (100ng/ml) for 24 hours. Cell proliferation was examined by the WST-1 (water-soluble tetrazolium salt) assay per Manufacture's protocol (Roche, Indianapolis, IN) followed by incubation with WST-1 reagent for 1, 2 and 4 hours. Absorbance at 450 nm was measured on a micro-plate reader (Bio-Rad). The experiment was done in triplicate, and repeated twice.

Tumor cell mediated osteolytic bone invasion model

4T1/Luc at 1×10^5 cells/50 μl was directly injected into the right tibia of 8-week old Balb/c mice as described (16). One week later, the animals were divided into two groups (10 mice per group) and received intravenously injection of AdExTek or AdGFP at 1×10^9pfu, respectively, as previously described (7). Bioluminescent activity was imaged in a cryogenically cooled IVIS-100 system (Xenogen, Alameda, CA) at 1 week and 2 weeks after the treatment, and photon counts were collected to reflect live tumor volume. At each time point, Radiographs of the lower extremity were obtained using an LX-60 cabinet digital x-ray system (Faxitron, Lincolnshire, IL). An exposure time of 5 seconds at 30 kVp was used. The percent of cortical destruction in the upper half of the tibia was calculated from the radiographic images using Image. For each tibia, the length was measured and the mid-point of the bone was marked. The linear extent of preserved cortex was measured (using the line tool) for both the anterior and posterior portions of the cortex and the two values were averaged together and the percent of cortical destruction calculated from that average.

Histology and immunohisochemistry

Animals were sacrificed at the end of the experiment. Hind limb bones were removed from mice and fixed in 10% formalin, decalcified in immunocal (Decal Chemical, Congers, NY) for 2 weeks, and then embedded in paraffin. Tissue sections from size matched tumors of two series experiments (n=10 mice/group) were stained with hematoxylin and eosin (H&E), and immunohistochemistry using anti CD31 antibody (Pharmingen) for vascular density measurement. Tissue sections from size matched tumors were also assessed for tartrate-resistant acid phosphatase (TRAP) activity, a marker for osteoclasts, as previously described (17). Positive staining was counted in ten randomly selected high power fields under microscopy and graphed.

Statistics

Results are reported as mean ± SE for each group. Statistical analyses were performed using two-tailed Student's t test for two-group comparison. Data were calculated with Statview 5.0 (Abacus Concepts, Berkeley, CA) statistical software. All tests of significance were two sided, and differences were considered statistically significant at $p<0.05$.

Results

Tie2 signaling directly regulates osteoclastogenesis

Osteoclast is derived from hematopoietic progenitor cells and Tie2 is present in these progenitor cells and important in hematopoiesis (10). In a previous study, we showed that neutralization of Tie2 signaling inhibited bone erosion in arthritis, suggesting a role of Tie2 in osteoclast differentiation (12). To test this hypothesis, we used an *in vitro* osteoclast differentiation assay from mouse ES cells as genetic manipulations of ES cells have been well established and a variety of knockout ES cells are available. After an induction of osteoclast differentiation from ES cells, we found a significant reduction of TRAP positive multinucleated osteoclasts developed from the Tie2 null cells compared to wild type cells (Figure 1A and 1B). To verify this finding, we used a biochemical approach, in which we induced osteoclast differentiation from wild type ES cell in the presence of recombinant soluble Tie2 protein (ExTek) to block Tie2 activation. Consistent with the genetic data, there was a significant inhibition of osteoclast differentiation in ExTek treated group compared to controls (Figure 1C and 1D). In addition, we did not observe any effect of ExTek on ES cell proliferation (Suppl Figure 1), which argues against toxicity plays a role in ES cell differentiation. Together, these results reveal a direct role of Tie2 signaling in osteoclast differentiation from progenitors.

These results were further corroborated using purified myeloid precursors from bone marrow. CD11b+ myeloid cells have the potential to differentiate into osteoclast and they are commonly used in osteoclastogenesis assays. CD11b+ myeloid cells are heterogeneous with respect to the expression of Tie2 (18). Therefore, we isolated CD11b+ myeloid cells from Balb/C mouse bone marrow using magnetic cell sorting. CD11b+ cells ($CD11b^{total}$) were further separated by flow cytometry into Tie2 positive ($Tie2^{+ve}$) and Tie2 negative ($Tie2^{-ve}$) cells. There were approximately 7.79% CD11b+ myeloid cells are Tie2 positive (Figure 2A). We achieved over than 98% purity of Tie2+ and Tie2− cells after cell sorting (data not shown), which were then used to induce osteoclast differentiation *in vitro*. After counting multinucleated cells (with 3 or more nuclei per cell), we found that Tie2 negative myeloid cells (CD11b+ Tie2−ve) form significantly fewer osteoclasts compared to Tie2+ myeloid cells (CD11b+ Tie2+ve) and total CD11b myeloid cells (Figure 2B and 2C). The osteoclast differentiation ability, fraction of plated cells that undergo differentiation, of Tie2+ and Tie2− CD11b myeloid cells are 1.1×10^{-3} and 0.6×10^{-3}, respectively. These data are consistent with early results and demonstrate a direct function of Tie2 signaling in osteoclastogenesis.

In addition, we also examined the potential role of Tie2 in osteoblastogenesis using ES cells. A few weeks of induction of ES cell differentiation, we did not observe any significant difference of Alizarin Red positive osteoclasts between wild type ES cells and Tie2 null ES cells (Figure 3A and 3B). Additionally, inhibition of Tie2 function using recombinant ExTek protein had no effects on osteoblast differentiation from wild type ES cells compared to control protein treated group (Figure 3C and 3D). These findings point to a specific role of Tie2 signaling in osteoclastogenesis, but not in osteoblastogenesis.

Neutralization of Tie2 function inhibited osteoclast formation and osteolytic bone invasion of mammary tumors *in vivo*

Since osteoclasts are critical for osteolytic bone metastasis and Tie2 signaling regulates osteoclast differentiation, we postulated that Tie2 signaling would be crucial for osteoclastogenesis in the mammary tumor-bone microenvironment. To address this question, we developed a 4T1 breast cancer cell line stably expressing luciferase (4T1/Luc) for non-invasive imaging. The 4T1 mouse mammary tumor cell line developed from Balb/c mice has several key advantages 1) it is one of only a few breast cancer models with the capacity to metastasize efficiently to sites affected in human breast cancer; 2) it resembles advanced breast cancer in humans and 3) is performed in an immunocompetent mouse.

We directly injected 4T1/Luc cells into the right tibia of 8-week-old female Balb/c mice. Upon the establishment of skeletal metastasis one week after tumor injection, the mice were randomly divided into two groups and received injection either AdExTek or control AdGFP through tail vein, respectively. Tumor growth was imaged by bioluminescent imaging one week and two weeks after the treatment (Figure 4A). There was a significant reduction of tumor volume reflected in the photon counts in animals that have received the ExTek treatment compared to controls (Figure 4B) (n= 10 mice/group, $p<0.05$).

At each time point, we also measured osteolytic bone destruction in live animals using digital X-ray radiography. At one week, the control tibias showed an average of 41.7% of the cortex of the upper tibia destroyed, while the treatment group showed an average of 15.0% of the cortex destroyed (Figure 5A and 5B) (n= 10 mice/group, $*p<0.05$). At two weeks, the control group showed an average of 61.8% of the cortex destroyed and the treatment group showed an average of 40.2% of the cortex destroyed (Figure 5C and 5D) (n= 10 mice/group, $*p<0.05$). Reduction of osteolytic bone destruction is consistent with the observation that Tie2 signaling plays a role in osteoclast differentiation.

Finally, we performed histological examination of tumor tissues in bone. We selected tissues from mice with similar-size tumors from each group to minimize/eliminate the potential impact of tumor burden on data analysis. We found that the cortical bone in the proximal tibias is largely destroyed and 4T1 cells are noted in the space between the remaining proximal and distal ends of the tibias. In contrast, there is limited cortical bone destruction in the ExTek treatment group (Figure 6A). Consistently, TRAP staining revealed significant fewer osteoclasts at the bone/tumor interface from ExTek treated animals than the one from control treated animals (Figure 6B and 6C). These findings are consistent with the assessment that Tie2 plays a role in osteoclast differentiation and neutralizing Tie2 function inhibited osteoclast differentiation and osteolytic bone erosion. In addition, we also examined tumor angiogenesis between the groups. CD31 staining showed a significant reduction of tumor vascular density when Tie2 function is blocked (Figure 6D and Suppl Figure 2), which correlates with increased necrosis in tumor section when compared to controls (Figure 6A). Taken together, these results support a role of Tie2 signaling in osteoclast differentiation and osteolytic bone invasion, in addition to tumor angiogenesis.

Discussion

Breast to bone metastases are predominately osteolytic in nature. While the metastasizing tumor cells invade the bone, osteoclasts in the area are stimulated to resorb bone and release growth factors that enable tumor cells to grow and progress in the local microenvironment. This reciprocal interaction between cancer cells and osteoclasts forms a vicious cycle that increases both bone destruction and the tumor burden (1). Therefore targeting osteoclast differentiation and breaking the vicious cycle offers an effective means to control bone metastasis. In this study, we reveal a critical role of Tie2, a mediator important in breast cancer angiogenesis, in osteoclastogenesis and osteolytic bone invasion. Neutralization of Tie2 activity inhibited the formation of osteolytic bone metastases and tumor growth of breast cancer. An understanding of molecular mechanisms underlying breast cancer bone metastases enhances the development of regimens to treat this disease.

Emerging evidence support a close association of angiogenesis with osteoclast formation and activity, and that endothelial cells stimulate osteoclastogenesis (19). In addition to the paracrine interaction of endothelial cells with osteoclasts, angiogenic mediators may directly regulate osteoclastogenesis and function. Osteoclasts are derived from hematopoietic stem cells and these cells are known to express certain endothelium specific receptors, such as VEGF receptor (VEGFR) and Tie2. Studies have shown that VEGFR-1 plays a predominant role in osteoclastogenesis and the maintenance of bone marrow functions (20). In this study, we demonstrate a direct function of Tie2 signaling specifically in osteoclastogenesis using both genetic and biochemical approaches. Deletion of Tie2 or inhibition of Tie2 activity impaired osteoclast development using an ES cell osteoclast differentiation assay, but has no effect on osteoblastogenesis. In addition, ExTek had no effects on ES cell proliferation. These data suggest a specific function of Tie2 in osteoclast differentiation, and argue against toxicity of ExTek affecting ES cell differentiation. In addition, we applied a commonly used osteoclastogenesis assay from bone marrow derived CD11b+ myeloid cells. Consistently, we found a significant reduction of osteoclastogenesis in Tie2− CD11b+ myeloid cells compared to Tie2+ myeloid cells. These data collectively reveal a direct function of Tie2 signaling in osteoclast differentiation.

Interestingly, although Tie2+ cells only account for less than 10% of total CD11b+ myeloid cells, the difference in osteoclastogenesis between total CD11b myeloid cells and Tie2+ myeloid cells is relatively small. This discrepancy may likely come from differences in levels of cytokines, such as angiopoietin, in culture conditions. It is likely that Tie2+ myeloid cells give rise to osteoclast, and Tie2− cells are a major supplier for the ligand. There exist multiple ligands for Tie2 and soluble Tie2 receptor likely binds all these factors. Based on the fact that angiopoietin-1 transgenic mice display increased bone formation (11), it is reasonable to assume that soluble Tie2 inhibits bone resorption likely through depletion of angiopotin-1.

In agreement with a role of Tie2 in osteoclast differentiation, blocking Tie2 activity using a soluble Tie2 receptor inhibited osteolytic bone invasion of breast cancer cells *in vivo*. We observed a 2.8 fold reduction of bone destruction one week after the injection of adenoviral vector expressing ExTek compared to controls, and the difference decreased to 1.5 fold at two weeks after the viral injection. This decrease of therapeutic index is likely due to a reduction of ExTek protein *in vivo*, as ExTek expression lasts for about one week to ten days after the viral injection in mice (7).

Moreover, we performed histological examination of tissue sections harvested from mice with similar size tumors to minimize the impact of tumor burden. We found that blocking Tie2 function using ExTek resulted in a significant reduction of osteoclast cells in addition to reduced tumor angiogenesis compared to controls. Accordingly, there was less bone

destruction and more necrosis in treated group than controls. Considering Tie2 is present in both endothelial cells and osteoclast precursors and Tie2 signaling regulates both angiogenesis and osteoclast differentiation, blocking Tie2 function could simultaneously inhibit tumor angiogenesis as well as osteoclast mediated osteolytic bone destruction.

In conclusion, this study identifies a novel function of Tie2 in osteoclastogenesis and osteolytic bone invasion of breast cancer. Taken together with previous findings, we would like to argue that Tie2 based inhibitors may have therapeutic benefits over the current treatment regiments for patients with metastatic breast cancer, i.e. bisphosphonates, since Tie2 signaling regulates not only angiogenesis, but also osteoclastogenesis. Neutralization of Tie2 function targets the stromal cells of the tumor microenvironment on multiple fronts, including tumor vascular development, inflammation and osteolytic bone metastasis. Tie2 is an important therapeutic target deserving further investigation.

Supplementary Material

Refer to Web version on PubMed Central for supplementary material.

Acknowledgments

We thank flow cytometry cores at Vanderbilt University Medical Center and VA, and Vanderbilt Immmunohistochemistry Core and Vanderbilt Institute of Imaging Sciences for technical support. This work is supported in part by grants from NIH (CA108856, NS45888 and AR053718).

Reference

1. Roodman GD. Mechanisms of bone metastasis. N Engl J Med 2004;350:1655–1664. [PubMed: 15084698]
2. Ribatti D, Nico B, Vacca A. Importance of the bone marrow microenvironment in inducing the angiogenic response in multiple myeloma. Oncogene 2006;25:4257–4266. [PubMed: 16518413]
3. Findlay DM, Haynes DR. Mechanisms of bone loss in rheumatoid arthritis. Mod Rheumatol 2005;15:232–240. [PubMed: 17029071]
4. Tanaka Y, Abe M, Hiasa M, et al. Myeloma cell-osteoclast interaction enhances angiogenesis together with bone resorption: a role for vascular endothelial cell growth factor and osteopontin. Clin Cancer Res 2007;13:816–823. [PubMed: 17289872]
5. Peters KG, Coogan A, Berry D, et al. Expression of Tie2/Tek in breast tumour vasculature provides a new marker for evaluation of tumour angiogenesis. Br J Cancer 1998;77:51–56. [PubMed: 9459145]
6. Lin P, Polverini P, Dewhirst M, Shan S, Rao PS, Peters K. Inhibition of tumor angiogenesis using a soluble receptor establishes a role for Tie2 in pathologic vascular growth. J Clin Invest 1997;100:2072–2078. [PubMed: 9329972]
7. Lin P, Buxton JA, Acheson A, et al. Antiangiogenic gene therapy targeting the endothelium-specific receptor tyrosine kinase Tie2. Proc Natl Acad Sci U S A 1998;95:8829–8834. [PubMed: 9671764]
8. Ash P, Loutit JF, Townsend KM. Osteoclasts derived from haematopoietic stem cells. Nature 1980;283:669–670. [PubMed: 7354855]
9. Suda T, Takahashi N, Martin TJ. Modulation of osteoclast differentiation. Endocr Rev 1992;13:66–80. [PubMed: 1555533]
10. Arai F, Hirao A, Ohmura M, et al. Tie2/angiopoietin-1 signaling regulates hematopoietic stem cell quiescence in the bone marrow niche. Cell 2004;118:149–161. [PubMed: 15260986]
11. Suzuki T, Miyamoto T, Fujita N, et al. Osteoblast-specific Angiopoietin 1 overexpression increases bone mass. Biochem Biophys Res Commun 2007;362:1019–1025. [PubMed: 17825261]
12. Chen Y, Donnelly E, Kobayashi H, Debusk LM, Lin PC. Gene therapy targeting the Tie2 function ameliorates collagen-induced arthritis and protects against bone destruction. Arthritis Rheum 2005;52:1585–1594. [PubMed: 15880817]

13. zur Nieden NI, Ruf LJ, Kempka G, Hildebrand H, Ahr HJ. Molecular markers in embryonic stem cells. Toxicol In Vitro 2001;15:455–461. [PubMed: 11566578]

14. Tsuneto M, Tominaga A, Yamazaki H, Yoshino M, Orkin SH, Hayashi S. Enforced expression of PU.1 rescues osteoclastogenesis from embryonic stem cells lacking Tal-1. Stem Cells 2005;23:134–143. [PubMed: 15625130]

15. Duplomb L, Dagouassat M, Jourdon P, Heymann D. Differentiation of osteoblasts from mouse embryonic stem cells without generation of embryoid body. In Vitro Cell Dev Biol Anim 2007;43:21–24. [PubMed: 17570030]

16. Fritz V, Louis-Plence P, Apparailly F, et al. Micro-CT combined with bioluminescence imaging: a dynamic approach to detect early tumor-bone interaction in a tumor osteolysis murine model. Bone 2007;40:1032–1040. [PubMed: 17251073]

17. Ballanti P, Minisola S, Pacitti MT, et al. Tartrate-resistant acid phosphate activity as osteoclastic marker: sensitivity of cytochemical assessment and serum assay in comparison with standardized osteoclast histomorphometry. Osteoporos Int 1997;7:39–43. [PubMed: 9102061]

18. De Palma M, Murdoch C, Venneri MA, Naldini L, Lewis CE. Tie2-expressing monocytes: regulation of tumor angiogenesis and therapeutic implications. Trends Immunol 2007;28:519–524. [PubMed: 17981504]

19. Cackowski FC, Roodman GD. Perspective on the osteoclast: an angiogenic cell? Ann N Y Acad Sci 2007;1117:12–25. [PubMed: 18056034]

20. Niida S, Kondo T, Hiratsuka S, et al. VEGF receptor 1 signaling is essential for osteoclast development and bone marrow formation in colony-stimulating factor 1-deficient mice. Proc Natl Acad Sci U S A 2005;102:14016–14021. [PubMed: 16172397]

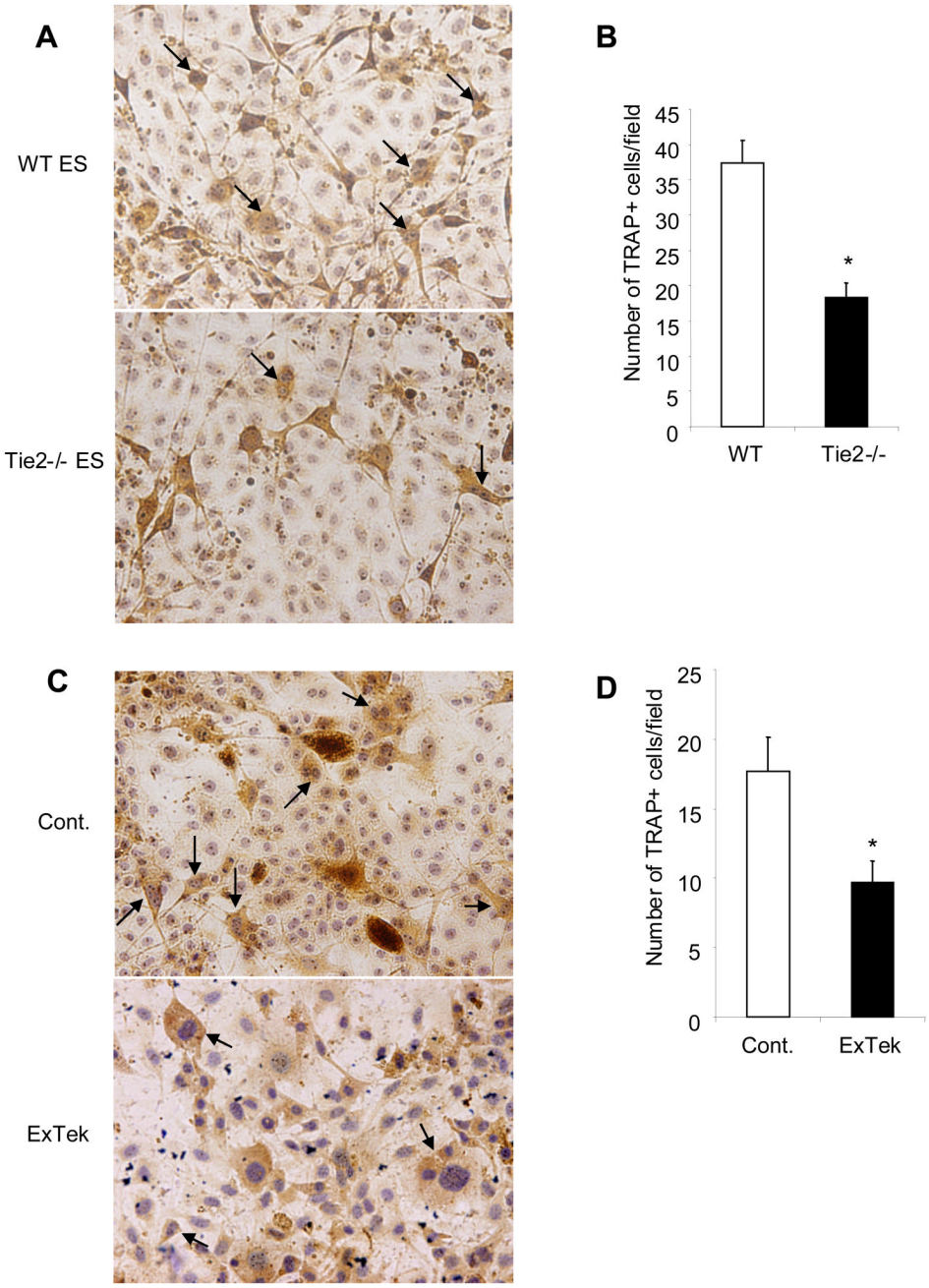

Figure 1. Tie2 signaling directly regulates osteoclastogenesis *in vitro*

TL1 ES cells and Tie2 null ES cells were induced differentiation toward osteoclast for approximately 3 weeks *in vitro*. TRAP staining was performed to detect matured multinuclear osteoclasts as marked by arrows (Panel A). Number of TRAP positive multinuclear osteoclasts were counted in randomly selected field under microscopy and graphed between wild type and Tie2 null ES cells (Panel B). The experiment was done in triplicate, and repeated three times. Results are mean ± SE. $^{*}p<0.05$ calculated with Statview 5. TL1 ES cells were induced differentiation toward osteoclast for approximately 3 weeks in the presence of recombinant ExTek at 100ng/ml or control protein. The media were replaced twice a week. TRAP staining was applied to detect matured osteoclasts as pointed by arrows (Panel C). Number of TRAP

positive cells were counted in randomly selected field under microscopy and graphed between the two groups (Panel D). The experiment was done in triplicate, and repeated three times. Results are mean ± SE. * $p<0.05$ calculated with Statview 5.

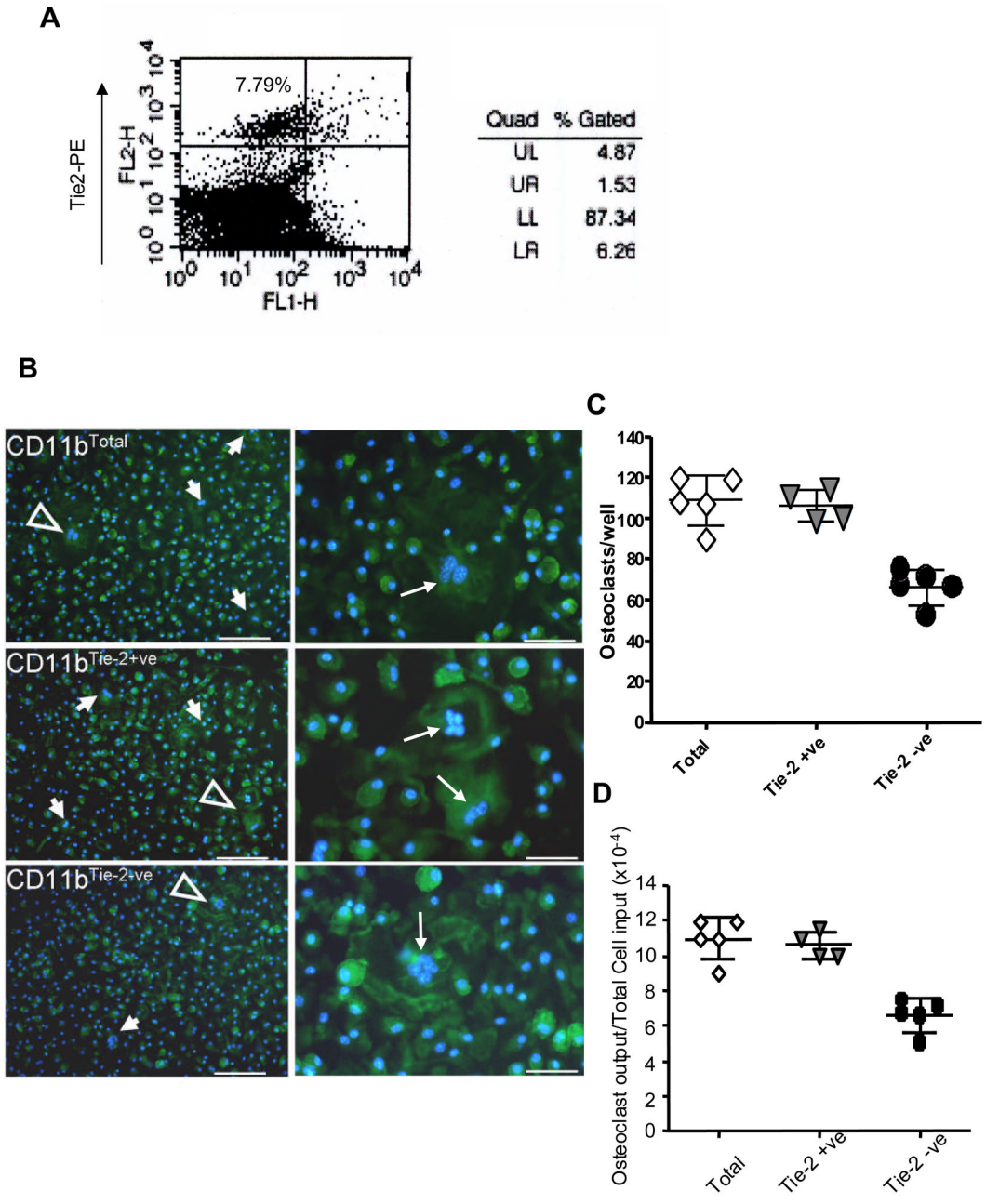

Figure 2. Tie2+ myeloid cell gives rise to osteoclast *in vitro*

CD11b positive myeloid cells were isolated from bone marrow of wild type mice by magnetic cell sorting. The cells were then stained with an anti Tie2-PE antibody and analyzed by flow cytometry for Tie2+ myeloid cells (Panel A). Tie2+ and Tie2− myeloid cell populations were isolated from CD11b+ myeloid cells by FACS sorting. These cells were subjected to induction of osteoclast differentiation for 3 weeks, followed by Actin ring staining. Actin ring positive (green) multinucleated (blue) osteoclasts were identified (arrow) in the $CD11b^{total}$, $CD11b^{Tie\text{-}2-ve}$ and $CD11b^{Tie\text{-}2+ve}$ group. Open arrows (Panel B, left panel) indicate areas of higher magnification (Panel B, right panel). Number of multinucleated osteoclasts (3 or more nuclei per cell) were counted in each well under microscopy and graphed (Panel C). These

experiments were done in triplicate and repeated on three independent occasions. $^{*}p<0.05$ between $CD11b^{Tie\text{-}2-ve}$ vs $CD11b^{Tie\text{-}2+ve}$ or $CD11b^{total}$. The osteoclast differentiation ability of $CD11b^{Tie\text{-}2-ve}$, $CD11b^{Tie\text{-}2+ve}$ and $CD11b^{total}$ myeloid cells were calculated and graphed (Panel D). These experiments were done in triplicate and repeated on three independent occasions. $^{*}p<0.05$ between $CD11b^{Tie\text{-}2-ve}$ vs $CD11b^{Tie\text{-}2+ve}$ or $CD11b^{total}$.

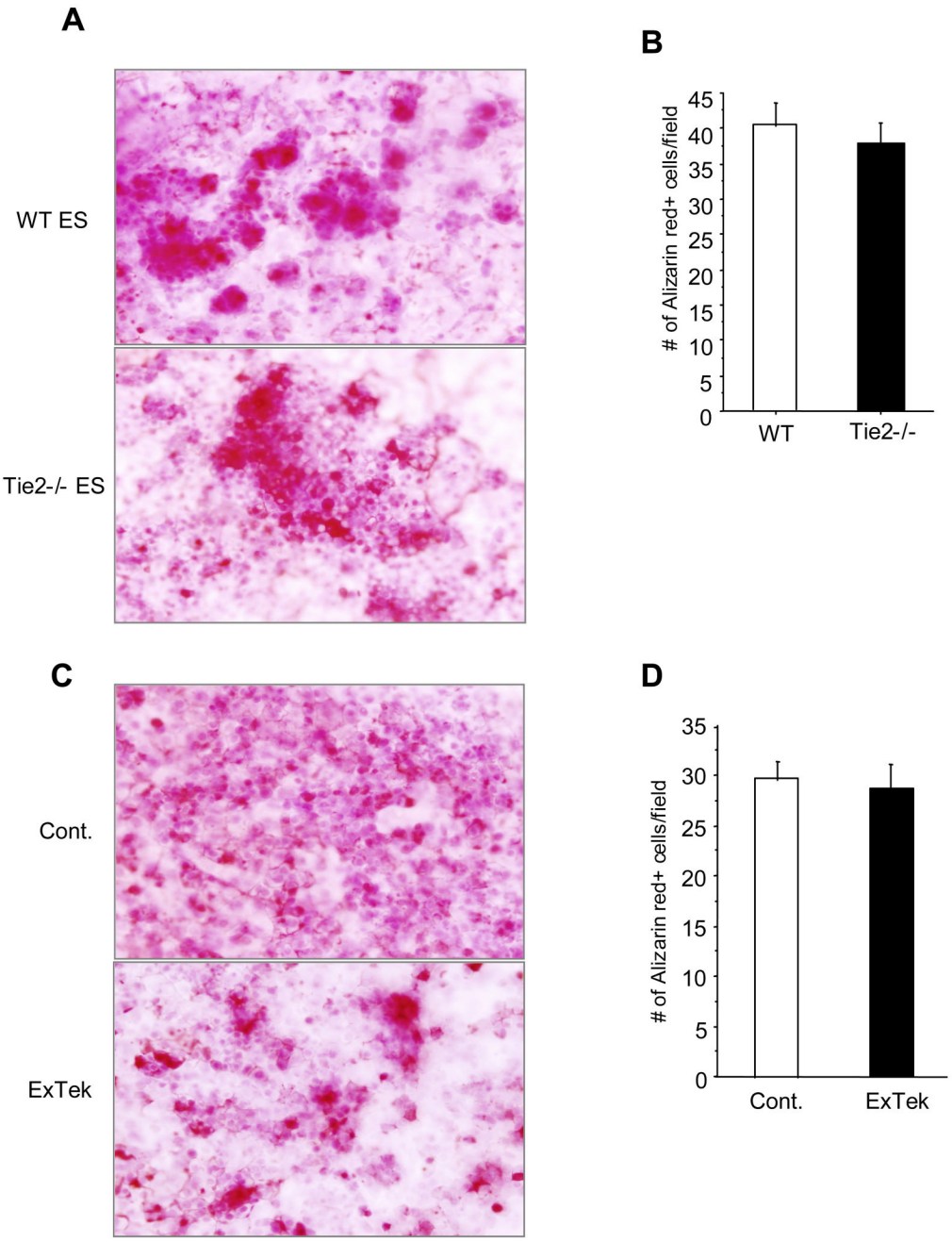

Figure 3. Genetic deletion of Tie2 had no effect on osteoblastogenesis *in vitro*

TL1 ES cells and Tie2 null ES cells were induced differentiation toward osteoblast for approximately 4 weeks *in vitro*. At the end of the experiments, cells were stained with Alizarin Red for osteoblasts (Panel A). Number of Alizarin Red positive cells were counted and graphed between wild type and Tie2 null ES cells (Panel B). Results are mean ± S.E. from three separate experiments. TL1 ES cells were induced to differentiate toward osteoblast in the presence of recombinant ExTek at 100ng/ml or control BSA protein (Panel C). Number of Alizarin Red positive cells were counted and graphed between the two groups (Panel D). Results are mean ± S.E. from three separate experiments.

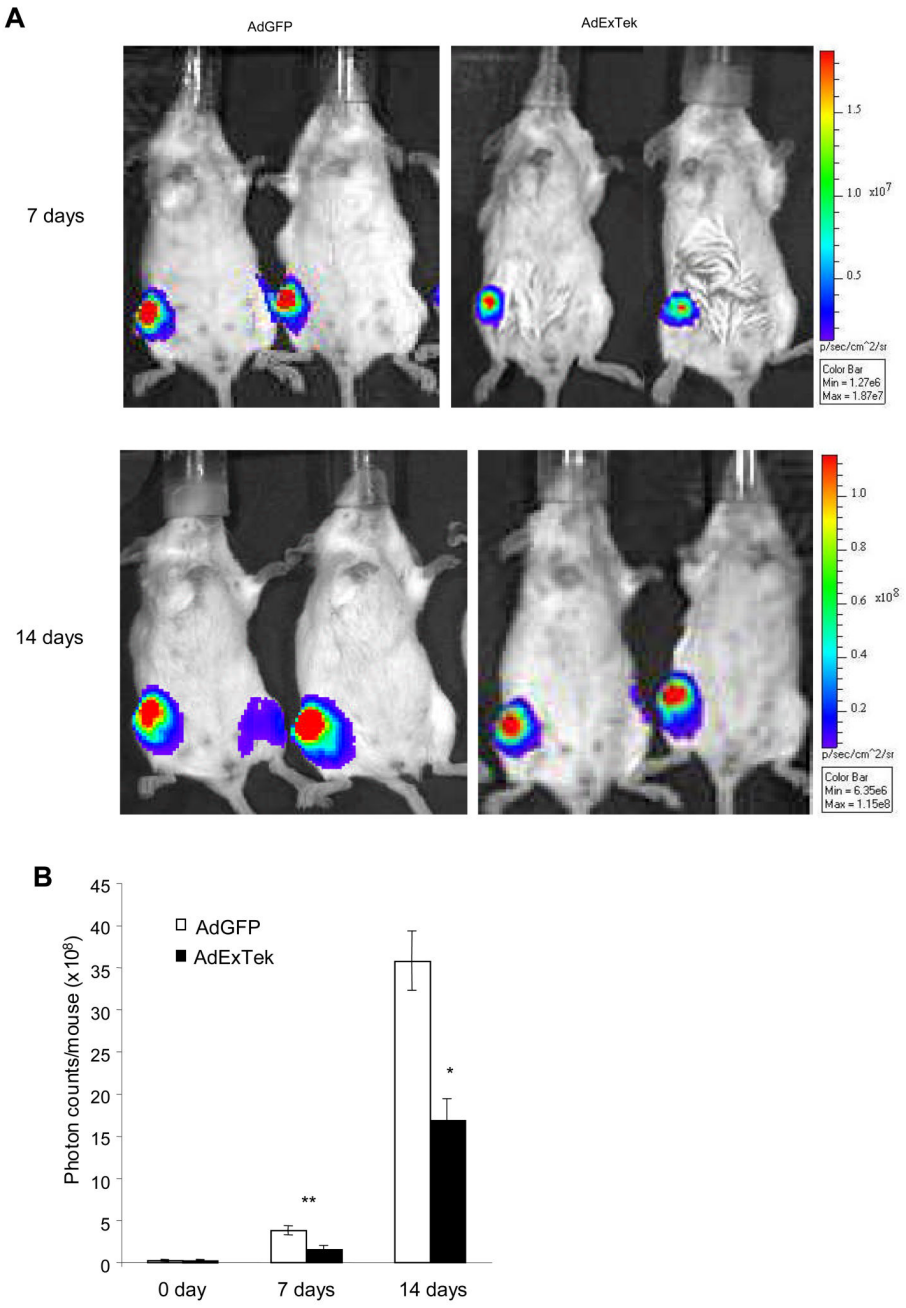

Figure 4. Neutralization of Tie2 function inhibited tumor growth in tibia bone

4T1/luc cells at 1×10^5 cells/50 μl/mouse were directly injected into the right tibia bone of 8-week old Balb/c mice. Seven days after tumor implantation, the mice were randomly divided into two groups and received either AdExTek or control AdGFP injection (10^9 pfu/mouse) via tail vein. Bioluminescence imaging was performed prior to the treatment, and one week and two weeks after the viral injection. Representative photos of mice over a 2-week period of time are shown (Panel A). Photon counts were collected at each time point in each group and graphed (Panel B). n=10 mice per group. The experiment was repeated once. Results are mean ± SE. *p<0.05, **p<0.01.

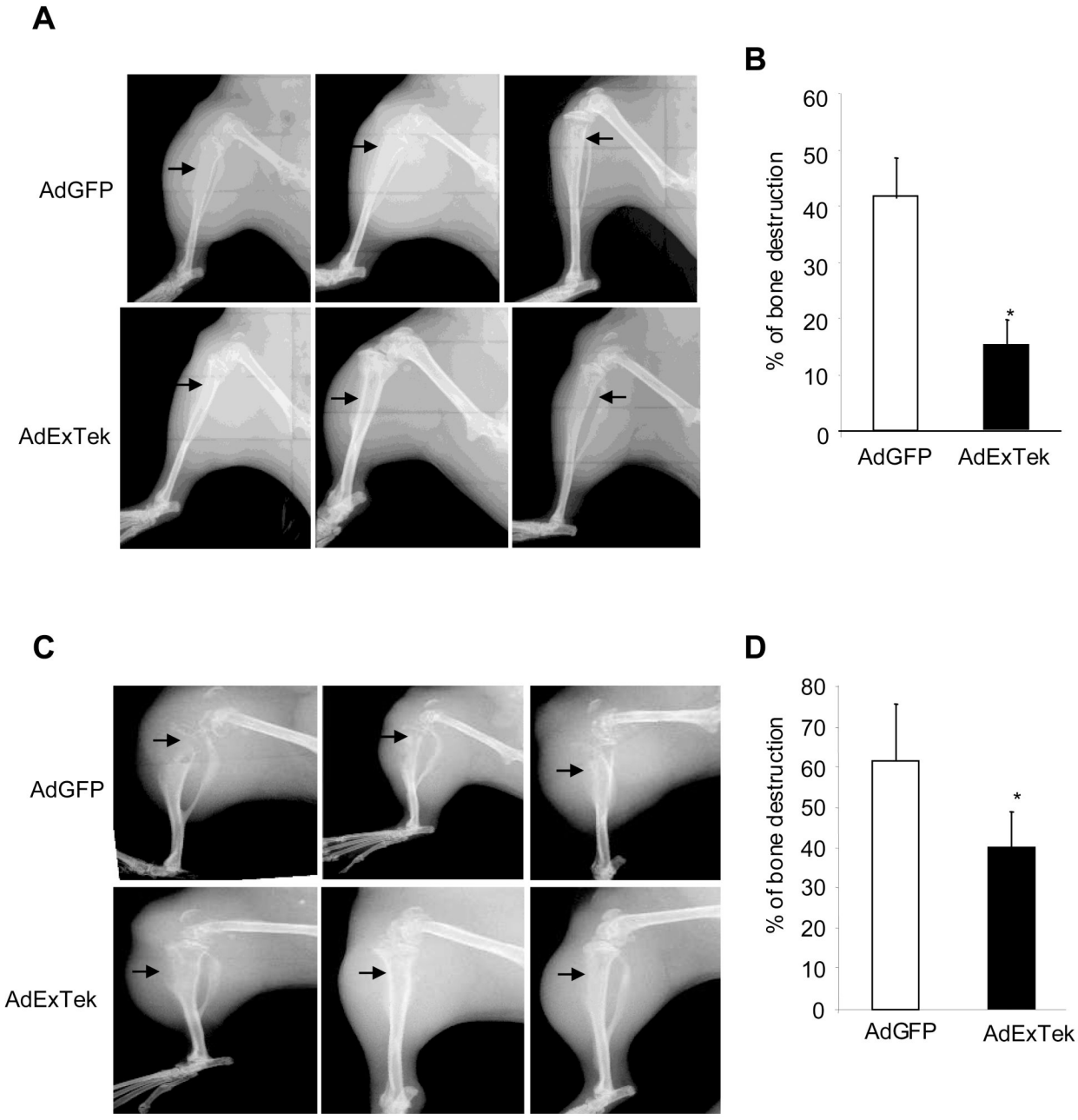

Figure 5. Neutralization of Tie2 function impaired osteolytic bone destruction *in vivo*

Bone destruction after tumor implantation was imaged using a Faxitron LX-60 digital x-ray system in live animals one week (Panel A) and two weeks (Panel C) after AdExTek and AdGFP injection. Representative radiographs of osteolytic lesions in hind limbs of Balb/c mice are shown. The percent of cortical bone destruction in the upper half of the tibia was calculated from the radiographic images using Image at 1 week (Panel B) and 2 weeks (Panel D) after the treatment. n=10 mice per group. The experiment was repeated once. Results are mean ± SE. *$p<0.05$.

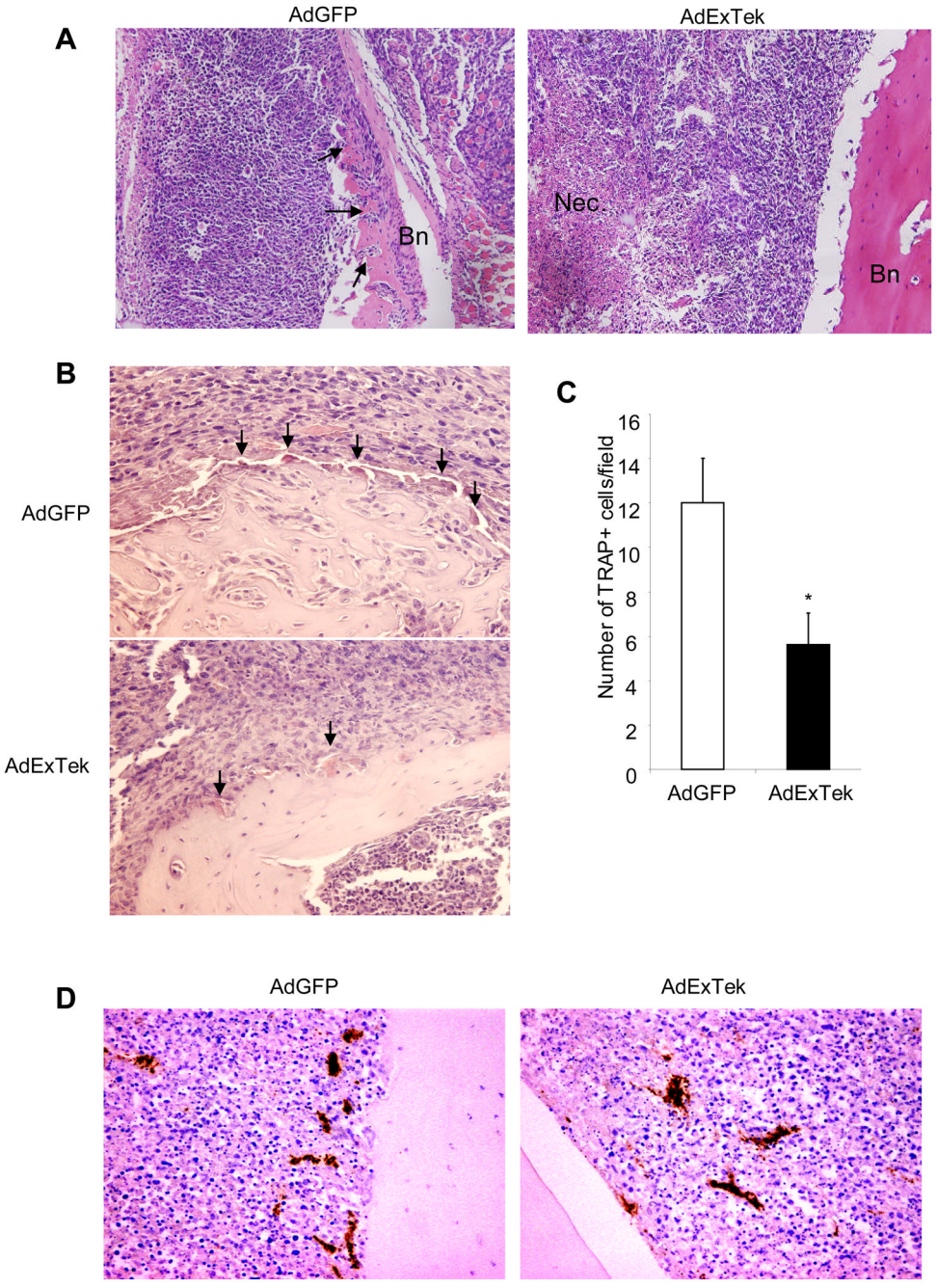

Figure 6. Histological evaluation of tumor-induced bone resorption

Tibia bone from size-matched control AdGFP and AdExTek treated groups was harvested three weeks after tumor implantation. Tissue sections were stained with HE to reflect histology and bone resorption. Representative images were shown. Bn represents bone, and Nec represents necrosis. Arrows point to tumor cell invasion and eroded bone. (Panel A). Tibia metastatic bone tissue from size-matched AdGFP and AdExTek treated groups were subjected to TRAP staining for osteoclast cells. Representative images of TRAP positive cells in tibia metastatic bone tissues are shown. Arrows point to osteoclasts (Panel B). TRAP positive cells were counted in 10 randomly selected fields under microscopy and graphed (Panel C). * $p<0.05$.

Tibia metastatic bone tissues were incubated with anti CD31 antibody for tumor vasculature (Panel D). Representative images were shown.